Journal of Biomedical Science (2007) 14:169–181
DOI 10.1007/s11373-006-9135-1

An IL-7 splicing-defect lymphopenia mouse model revealed by genome-wide mutagenesis

Hong-Wen Huang[1], Yun-Jung Chiang[1], Shuen-Iu Hung[2], Chung-Leung Li[3] & Jeffrey Jong-Young Yen[1,*]

[1]*Institute of Biomedical Sciences, Academia Sinica, No. 128, Sec.2, Yen-Jiou-Yuan Rd., Taipei, 11529, Taiwan;* [2]*Genotyping Center, Genomics Research Center, Academia Sinica, Taipei, 11529, Taiwan;* [3]*Stem Cell Program, Institute of Cellular & Organismic Biology/Genomics Research Center, Academia Sinica, Taipei, 11529, Taiwan*

Received 10 January 2006; accepted 25 October 2006

Key words: IL-7, ENU mutagenesis, phenotype screening, lymphopenia

Abstract

Homeostasis of the hematopoietic system is tightly regulated by an array of cytokines that control proliferation, differentiation and apoptosis of various cell lineages. To identify genes that are essential for hematopoietic homeostasis, we screened C57BL/6 mice that had been genome-wide mutagenized by *N*-ethyl-*N*-nitrosourea (ENU) to produce altered blood cell composition. We identified a mutant mouse line with a drastic reduction in the number of T and B cell lineages in lymphatic tissues and peripheral blood, as well as severe atrophy of the thymus and lymph nodes. Genotyping with a genome-wide single nucleotide polymorphism (SNP) marker set mapped the mutant phenotype to chromosome 3A and subsequent direct DNA sequencing revealed a G-to-A point mutation in the splicing donor site of the third exon of the candidate gene for IL-7, a lymphocyte survival cytokine. Such mutation resulted in skipping of exon 3 and production of an internally truncated IL-7 (ΔE3-IL7). Furthermore, using recombinant proteins produced in a baculoviral system, we demonstrated that ΔE3-IL7 had no detectable anti-apoptotic activity even at a dose that was 30 times more than that required for a wild-type protein to manifest a full activity in a naïve T cell survival assay. Our data suggest that this mutant mouse line provides an alternative animal model for the study of severe combined immunodeficiency (SCID) syndrome in humans.

Introduction

The hematopoietic system is a highly sophisticated system, in which a single stem cell propagates and differentiates into numerous cell types, including red blood cells, platelets, lymphocytes, monocytes and granulocytes. In addition to cell–cell interaction signals, this process is tightly regulated by an array of cytokines that control proliferation, differentiation and apoptosis of hematopoietic lineages. The use of gene targeting techniques has been very powerful in confirming the importance of cytokines and intermediate signaling molecules in homeostasis maintenance of the hematopoietic system. Specifically, gene targeting has enabled researchers to produce a clean and definite elimination of certain gene products in a physiological context, and thus has allowed the role of these molecules to be addressed. However, gene-driven genetic ablation approaches frequently encounter several problems when knockout animals are used as models for human disease. These problems

*To whom correspondence should be addressed. Fax: +886-2-2782-9142; phone: +886-2-26523077; E-mail: bmjyen@ibms.sinica.edu.tw

include the lack of homozygotic offspring due to embryonic lethality, the lack of consistency with prior observations due to the emergence of novel phenotypes and the propensity for knockout mice to mount immune reactions to wild-type gene products. ENU is a super-efficient germ cell mutagen. Combining ENU mutagenesis with the mouse genome sequence annotation that is now available [1] has enabled phenotype-driven screening of genome-wide ENU-mutagenized mice to be achieved on a large scale in complicated systems such as hematopoiesis. This technique constitutes an affordable complementary approach [2–5] and has aided the discovery of novel gene components involved in the circadian cycle, LPS signaling and T cell activation [6–8].

IL-7 was initially identified and cloned as a stromal cell-derived B cell proliferation factor [9] and was subsequently shown to be a growth and survival factor for mature and immature thymocytes [10]. IL-7 is produced by both immune and non-immune cells, including B-cells, monocytes, macrophages, follicular dendritic cells, stromal cells, gut epithelial cells and keratinocytes [11]. Gene targeting studies in mice revealed that IL-7 plays a critical role in lymphopoiesis, as the peripheral blood and all lymphatic tissues of IL-7 null mice were found to be highly lymphopenic [12]. Recent research suggests that the IL-7/IL-7 receptor α/receptor γc/Jak3 signaling pathway is by far the most important cytokine pathway required for lymphocyte development and homeostasis. Animals defective in IL-7 and the IL-7 receptor [12, 13] as well as patients with defective γc, Jak3 and IL-7 receptors [14–18] show severe lymphopenia and suffer from severe combined immunodeficiency (SCID) syndrome.

In the present study we show that large-scale screening of ENU mutagenized mice can efficiently identify a lymphopenia mouse model for the human SCID disorder. Furthermore, the powerful genome-wide high density SNP marker genotyping facility is useful in rapidly mapping the chromosomal location of the disease allele. Finally, genomic sequencing and molecular biology studies revealed that we have obtained a mutant mouse line that contains a point mutation at the splicing donor site of the IL-7 gene, which results in skipping of the third exon, producing a seemingly inactive IL-7, and conferring severe lymphopenia phenotype on mutant animals.

Materials and methods

Generation of ENU-recessive mice

A three-generation breeding scheme of ENU-mutagenized mice for recessive mutant phenotype was adopted as described previously [19]. These studies were reviewed and approved by the Institutional Animal Care and Utilization Committee of Academia Sinica.

Complete blood cell counting (CBC) with Cell-Dyn 3700

Approximately 300 μl of anti-coagulated whole blood from the tail vein was analyzed with a CELL-DYN 3700 (Abbott Diagnostics).

Flow cytometric analysis of surface markers

Cells were isolated from peripheral blood, bone marrow, thymus, lymph node and spleen by standard procedures. Approximately 1 million viable cells were labeled by incubating with various antibodies for 30 min on ice. PE-conjugated mAbs were directed against CD4 and B220. FITC-conjugated mAbs were against CD8 and Gr-1; APC-conjugated mAbs were against TCRβ and CD11b. All antibodies were purchased from e-BioScience (San Diego, CA) except anti-TCRβ antibody (BD Pharmingen). Cell surface immunofluorescence analysis was performed using a cell sorter (Vantage; Becton Dickinson Immunocytometry Systems, San Jose, CA). Annexin V staining of apoptotic cells (BioVision Research) was performed according to the vendor's instruction as previously described [20, 21].

Genomic DNA sequencing

Genomic DNA was isolated from 0.5-cm tail clippings using a PUREGENE DNA purification system (Gentra systems, Minnesota, USA). A 300 ng sample of DNA was then subjected to PCR amplification for 42 cycles. The following primers were used to amplify the third exon of the IL-7 gene: 7E3F: 5′-cattgatgccagtaagtagaatcagg-3′; 7E3R: 5′-gtatctcctggagacagggtgtctg-3′. The final PCR product was then subjected to direct sequencing with PCR primers.

SNP genotyping

A genome-wide mouse SNP data set containing 10,915 SNPs of 48 mouse strains was kindly provided by Tim Wiltshire (Genomics Institute of the Novartis Research Foundation) [22]. A total of 276 SNPs were selected for genotyping, according to the determined criterion: the genotype of the mouse strain C3H/HeJ was different from that of C57BL/6J. The average space between the SNPs was 10 Mb. SNP genotyping was performed by high-throughput MALDI-TOF mass spectrometry [23, 24]. Primers and probes flanking the SNPs were designed in multiplex format using SpectroDESIGNER software (Sequenom, San Diego, CA, USA). Genotyping experiments were performed as described previously [25].

RT-PCR and quantitative RT-PCR

Total RNA was isolated from thymus of both affected and unaffected mice using the Trizol® RNA isolation kit (Invitrogen, Carlsbad, CA). A 3-μg sample of RNA was then subjected to reverse transcription reaction with superscript III RTase (Invitrogen). Half microgram aliquots of cDNA were used as the template for conventional PCR reactions. The following primers used for studying the alternative splicing of the exon 3: Exon 2F: 5′-tctttggaattcctccactgatcc-3′; Exon 3F: 5′-acaggaactgatagtaattgcccg-3′; Exon 4R: 5′-actgtgcagttcaccagtgtttg-3′. Quantitative RT-PCR was performed with an ABI PRISM 7700 Sequence Detection System using CYBR as the fluorescent dye following the manufacturer's protocol (ABI). The following primers used for the exon 4 or 4/5 quantitation: Exon 4F: 5′-aagctgctttctaaatcgtgctg-3′; Exon 4R: 5′-acttgtgcagttcaccagtgtttg-3′; Exon 4/5F: 5′-atcagtgaagaattcaatgtc-3′; Exon 4/5R: 5′-ctttaggaaacatgcatcattc-3′. GAPDH was chosen as the internal control and its primers were gapdh-F: 5′-tgcaccaccaactgcttag-3′ and gapdh-R: 5′-gatgcagggatgatcttc-3′, as described previously [26]. Analysis of the results was based on the *Ct* calculation [27], where *Ct* represents the cycle number at which fluorescence intensity of the PCR products reach a given threshold.

Production of recombinant IL-7 and ΔE3-IL-7

Full-length IL-7 and ΔE3-IL-7 cDNA were obtained from wild-type and affected thymic mRNA by RT-PCR. The primers used to obtain the complete coding sequences were as follows: IL-7start: 5′-ggatcccgcagaccatg-3′; IL-7stop: 5′-gatatccatgtcctgttta-3′. The PCR products were sequence-verified, subcloned into the transfer vector pVL1393. The recombinant baculovirus was generated in the SF21AE insect cells according to a protocol recommended by the manufacturer (BD PharMingen Inc.). Conditioned media to be used in the naive T cell survival assay (see below) were collected from insect cells infected with recombinant virus producing wt or mutant IL-7 or an irrelevant protein (XylE) provided in the BaculoGold kit. The amount of IL-7 (wt or mutant) present in the conditioned medium was subsequently analyzed by Western blot with anti-mouse IL-7 antibody (BAF407, R & D Systems, Inc.) as previously described [21], or quantified by the enzyme linked immunosorbent assay (ELISA) according to vendor's instructions (R & D Systems Inc.).

Biological activity of IL-7 determined by a naive T cell survival assay

The biological activity of recombinant IL-7 (wt or mutant) was determined as described previously [28]. In brief, naïve splenic T cells from C57BL/6 mice were first positively selected with CD90 (Thy1.2) microbeads on an LS column (Miltenyi-Biotech) according to the manufacture's instructions. The selected T cells were cultured in RPMI1640 medium supplemented with 10% fetal bovine serum (Gibco) and various doses of conditioned media containing wt- or ΔE3-IL7. Four days later, dead cells under each treatment were quantified by an annexin V-Cy3 apoptosis detection kit (BioVision).

Results

Identification of a lymphopenia phenotype

Many gene-targeted mice in which gene products that play an important role in hematopoietic system development have been developed. The

generation of these mice has enhanced researchers' ability to investigate the physiological functions of these genes and has aided in the development of models for human genetic diseases. However, animal models generated from gene ablation do not perfectly mirror the effects of naturally occurring human diseases. In order to create a more physiological disease model and potentially discover a novel regulator of the hematopoietic system, we have screened genome-wide ENU mutagenized mice for peripheral blood cellular abnormalities. Initially, several potential phenotypes were considered and in one of the candidate mutant lines, the same phenotype was identified in multiple offspring from the same G2 mother, for example G3-023 and G3-026 (Figure 1), suggesting the existence of a heritable trait. The average white blood cell (WBC) number decreased from the normal level of $\sim 8 \times 10^6$ cells/ml to $\sim 1.5 \times 10^6$ cells/ml in affected offspring and the lymphocyte (LYM) number decreased from $\sim 7 \times 10^6$ cells/ml to $\sim 0.5 \times 10^6$ cells/ml, without significantly altering the number of myeloid cells. To further test the heritability of the mutant phenotype, two of the affected animals, G3-023 and G3-026, were initially mated to C57BL/6 mice (Figure 1, G3-023) to produce a heterozygous G4 generation. G4 animals were then intercrossed to generate the G5 generation in order to determine the trait's heredity as a recessive phenotype (Figure 1). To explore the penetrability of this recessive phenotype in different genetic backgrounds, G3 were also outcrossed with C3H/HeJ (Figure 1, G3-026) to generate heterozygous N1 animals that in turn were intercrossed to produce the N1F1 generation. The target phenotype (Figure 1) was identified repeatedly in multiple G5 animals such as G5-B-32, G5-B-33 and the N1F1 generation (N1F1-C-50). Our data suggest that the mutation accounts for the lymphopenia phenotype is heritable and expressed in both BL/6 and C3H mouse strains. Approximately 20% of the offspring from G4 and N1 intercrosses acquired the affected phenotype (data not shown), further suggesting that the underlying mutation behaves as a recessive genetic trait with near complete penetrability.

Combined T and B cell deficiency in mutant animals

Affected mice show normal behavior, activity, development, body weight, and a normal survival curve under the SPF breeding environment. To begin to elucidate the mechanism that accounts for the lymphopenia phenotype, general morphological inspection and necropsy were performed. The mutant mice were generally free of readily apparent physiological defects, except that the thymus (Thy) and lymph nodes (LN) were severely atrophic; additionally, a slight reduction in the weight of the spleens (SP) was noted (Figure 2A). Consistent with the gross inspection of size and weight, the number of cells in the LN and Thy was greatly reduced, by 10- to 20-fold, while only a slight reduction was seen in the SP and peripheral blood (PB) (Figure 2B). Although total cell number in PB was only slightly decreased (Figure 2B), flow cytometric analysis of white blood cells revealed that TCRβ^+ T cells (both CD4+ and CD8+) decreased from 18 to 2% and B220$^+$ B cells decreased from 27 to 1%. Although CD11b$^+$/Gr-1$^+$ myeloid cells increased from 37 to 93% (Figure 3A), their total number in affected versus unaffected mice remained largely unchanged (Figure 3B). This was also true for the bone marrow and spleen in that

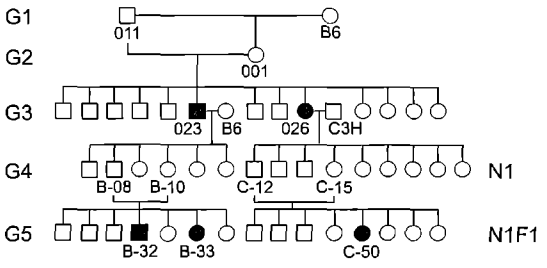

Figure 1. Identification of a lymphopenia mutant mouse line. This line was founded by a male G1-011 and its daughter G2-001. This pair produced several litters of G3 mice, including an affected male mouse, G3-023, and an affected female mouse, G3-026. These two animals were mated with both C57BL/6 (B6) and C3H/HeJ (C3H) mice to produce G4 and N1 generations, respectively. B-08 and B-10 of the G4 generation were mated to produce the G5 generation wherein two affected mice, B-32 and B-33, were identified. On the other hand, C-12 and C-15 of N1 generation were mated to generate the N1F1 generation, from which one affected female C-50 was identified. Solid squares and circles indicate affected animals.

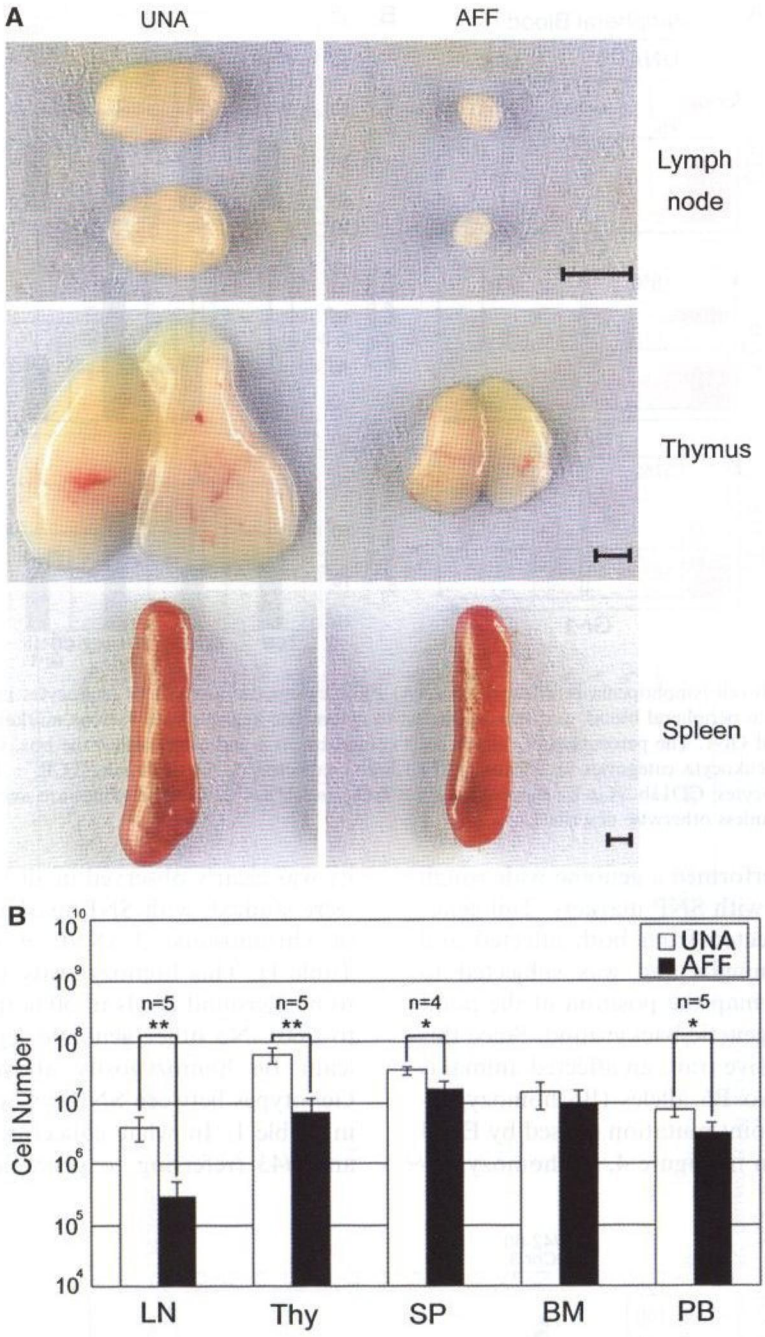

Figure 2. Thymus and lymph node atrophies in affected mouse. (**A**) Gross appearance of lymph nodes, thymus and spleen of affected (AFF) and unaffected (UNA) mice. The bars in the picture represent the size of 1 mm. (**B**) The total cell numbers of five major lymphatic compartments. LN: lymph node; Thy: thymus; SP: spleen; BM: bone marrow; and PB: peripheral blood. $*p < 0.05$; $**p < 0.001$. "*n*" indicates the animal numbers. The values are average ± SD of four independent measurements, unless otherwise described.

the number of T and B cells was dramatically reduced, about 10- to 20-fold, whereas the number of $CD11b^+/Gr\text{-}1^+$ (neutrophils and granulocytes) and $CD11b^+/Gr\text{-}1^-$ (monocytes) populations remained unchanged (Figure 3B).

Identification of a point mutation at the IL-7 gene

To examine the molecular mechanism mediating this lymphopenia phenotype and to further explore the molecular identity underlying this

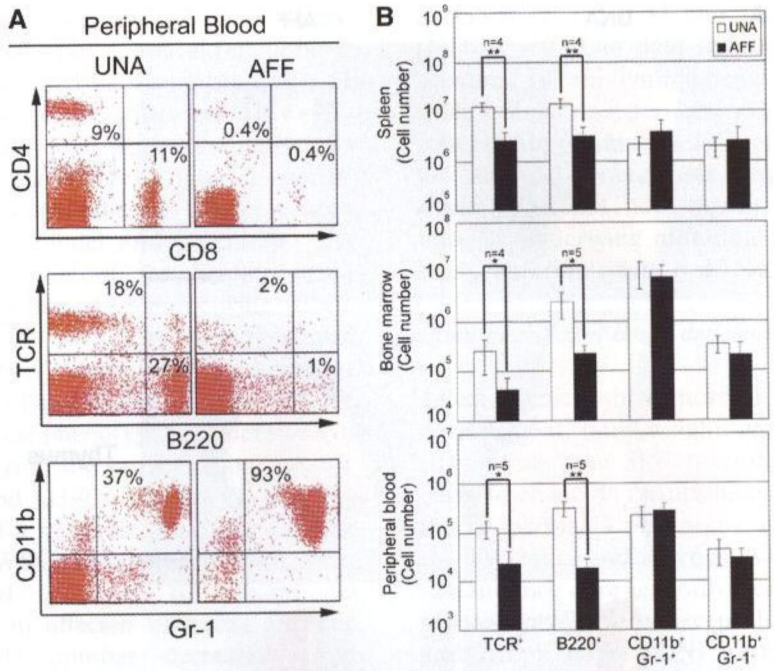

Figure 3. Severe T and B cell lymphopenia in affected mice. (**A**) Flow cytometric analysis of leukocytes in peripheral blood. Leukocytes were isolated from peripheral blood, and then subjected to cytometric analysis with various markers, including CD4, CD8, TCRβ, B220, CD11b and Gr-1. The percentage of cells in each compartment is indicated within the box. (**B**) Differential cellularities of the four major leukocyte categories in affected (AFF) and unaffected (UNA) animals. TCR^+: T cells; $B220^+$: B cells; $CD11b^+/Gr\text{-}1^+$: granulocytes; $CD11b^+/Gr\text{-}1^-$: monocytes. $^*p < 0.05$; and $^{**}p < 0.001$. The values are average ± SD of four independent measurements, unless otherwise described.

genetic defect, we performed a genome-wide rough mapping procedure with SNP markers. Tail genomic DNA was collected from both affected and unaffected N1F1 animals and was subjected to genotyping so as to map the position of the point mutation in the B6 genetic background. Since this phenotype is a recessive trait, an affected animal is expected to have two B6 alleles (B6 homozygosity), at or near the point mutation caused by ENU treatment. As shown in Figure 4, B6 homozygosity was clearly observed in all 15 affected mice that were studied, with SNP markers at the 3A region of chromosome 3 (SNP # 42 and #43; also Table 1). This homozygosity gradually decreased to background levels of 50% frequency (from #44 to #60). No other genomic region showed significant B6 homozygosity above 80% (Figure 4). Genotypes between SNP # 42 and # 53 are shown in Table 1. In what concerns SNP markers #42 and #43 (referring to genomic positions at 5.65

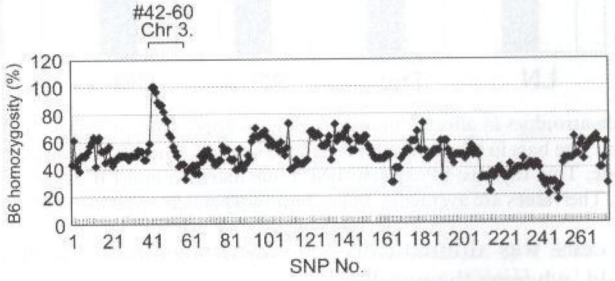

Figure 4. Whole genome screening of 276 SNPs for lymphopenia. On the *x*-axis, 276 SNPs are ordered by their chromosomal positions, including 19 SNPs (SNP #42–60) located on chromosome 3. The percentages of homozygosity with the B6 allele background were calculated among the affected mice and are shown on the *y*-axis. Two consecutive SNPs (SNP #42, 43) located terminal to the A region of chromosome 3 show 100% of the B6 alleles.

Table 1. SNP allele frequency of 15 affected lymphopena mice.

Chromosome		3											
Position (Mb)[a]		5.65	8.47	15.28	28.43	47.92	51.02	56.45	62.32	73.6	85.16	90.27	101.36
SNP No.[b]		42	43	44	45	46	47	48	49	50	51	52	53
NCBI ID.		rs13476957	rs13476965	rs13476986	rs13459183	rs13477095	rs13477105	rs4223969	rs13477147	rs6289734	rs6183172	rs13477252	rs13477292
Animal ID	B6	A	G	C	T	T	T	A	T	A	G	A	T
	C-036	A	G	C	TC	CT	AT	C	A	–	A	G	C
	C-039	–	G	–	T	T	T	AC	AT	AT	–	GA	CT
	C-034	A	G	C	–	T	T	A	T	A	G	A	T
	C-033	A	G	C	T	CT	AT	–	AT	T	A	G	C
	C-092	A	G	TC	C	C	A	C	A	T	A	G	C
	C-098	A	G	C	T	T	T	A	T	AT	GA	GA	CT
	C-099	A	G	C	T	T	T	A	T	A	G	A	T
	C-100	A	G	C	T	T	T	A	T	A	G	A	T
	C-102	A	G	C	T	T	T	A	T	A	GA	GA	CT
	C-032	A	G	C	T	T	T	A	T	A	G	A	T
	C-217	A	G	C	T	T	T	A	T	A	GA	GA	CT
	C-218	A	G	C	T	T	T	A	T	A	G	A	T
	C-221	A	G	C	T	T	T	A	T	A	G	A	T
	C-306	A	G	C	T	T	T	A	T	A	G	A	CT
	C-311	A	G	C	T	T	T	A	AT	AT	–	GA	C
Homozygosity (%)		100	100	96.4	89.3	86.7	86.7	82.1	76.7	75	65.4	63.3	56.7

[a]SNP positions along chromosome 3 are derived from Ref. [19].
[b]The serial number of the 276 SNP markers used in this experiment.

and 8.47 Mb of chromosome 3) [22], all affected animals invariably contained the B6 alleles and no C3H alleles. The percentage of B6 homozygosity decreased for other markers in chromosome 3, from 96.4% (#44) to 89.3% (#45), to 86.7% (#46 and #47), 82.1% (#48), 76.7% (#49), 75% (#50), 65.4% (#51), 63.3% (#52), and eventually to 56.7% (#53). These data strongly suggest that the point mutation introduced into the B6 genome by ENU mutagenesis is most likely located between markers 42 and 43, within a 2.8 Mb interval. We determined the genotypes of 80 additional affected N1F1 mice (lymphocyte counts $\leq 1.5 \times 10^6$ per ml) with the SNP #42 marker; 79 out of 80 animals displayed B6 homozygosity (data not shown), one animal was heterozygous. Furthermore, the genotypes of 125 unaffected N1F1 animals (lymphocyte counts $\geq 2 \times 10^6$ per ml) were also determined. Only one out of 125 unaffected animals had homologous B6 alleles (data not shown). Our genotyping data strongly suggest that the mutant phenotype is physically strongly associated with SNP marker #42.

We then asked if there was a mutation or deletion of any known gene located within this genomic region of mouse chromosome 3 that results in immune system defects similar to that seen in our mutant mice. A search of the database for immune system phenotypes at the Jackson Laboratory website (The Phenotypes and Alleles program of Mouse Genomic Informatics), revealed two targeted alleles of the IL-7 gene fulfilled our criteria. As IL-7 is one of the major cytokines essential for T and B cell survival and lymphatic organ development [12], and IL-7 knockout mouse phenotypes are very similar to what we observed in our mutant mice, although the knockouts are more severe, we investigated the sequence of every IL-7 coding exon and exon/intron junction. The genomic DNA of an affected mouse and a control inbred C57BL/6 mouse was subjected to PCR, with primer pairs flanking all five exons of the IL-7 gene (data not shown). The PCR fragments were then subjected to sequencing reactions using those PCR primers. All but one of sequences of the affected animal were identical to those of the control animal. There was one cytosine nucleotide at the exon 3 splicing junction that had been changed to a thymine nucleotide in the affected animal when we used the reverse primer (Figure 5A). To further confirm that this alteration was indeed tightly associated with the mutant phenotype, the sequence of the exon 3 splicing junction was also determined for the N1 heterozygotic animal. As shown in Figure 5A, the genotype of this nucleotide was C/T, which is consistent with our hypothesis.

Production of aberrant IL-7 mRNA and protein

To investigate whether this mutation alters IL-7 gene expression, IL-7 mRNA expression in control and mutant mice was analyzed. Thymic RNA was prepared and subjected to RT-PCR with a primer pair located within exon 3 and 4, respectively (arrows, Figure 5B). As shown in Figure 5C, while RNA from the unaffected animal gave a predicted 190-bp DNA fragment (lane 1), which was confirmed by subcloning and sequencing (data not shown), there was no apparent PCR product that could be identified with RNA from the affected animal (lane 2). This was likely due to the exclusion of exon 3 from the mature mRNA. Therefore, we repeated the same RT-PCR experiment using another primer pair, located at exon 2 and 4 (Figure 5B). Once again, the RNA of the unaffected animal produced a DNA product of the predicted size of 310-bp (lane 3). However, a 248-bp DNA fragment (lane 4), rather than 310-bp, was obtained with mRNA of the affected animal. Direct sequencing of this fragment (data not shown) revealed that exon 2 was directly spliced to exon 4; supporting the hypothesis that exon 3 skipping had occurred in the affected animal (ΔE3 IL-7 mRNA, Figure 5B). Since splicing of aberrant RNA molecules is usually less efficient, we then utilized real time quantitative RT-PCR to investigate the possible reduction of this aberrant mRNA in thymus. As shown in Figure 6, the level of IL-7 mRNA was determined by a primer pair that amplified the sequence across exons 4 and 5 (right panel) or the exon 4 alone (left panel). Consistent with the results shown in Figure 5C, the IL-7 mRNA level of affected mice was not significantly different from that of the unaffected animal, regardless which set of primer was used ($p = 0.29$ for exon 4, and $p = 0.35$ for exon 4/5, both $p > 0.05$). These data suggest that the point mutation at the splicing junction caused aberrant splicing of the mutant IL-7 precursor RNA, but had no effects on the efficiency of such a splicing event.

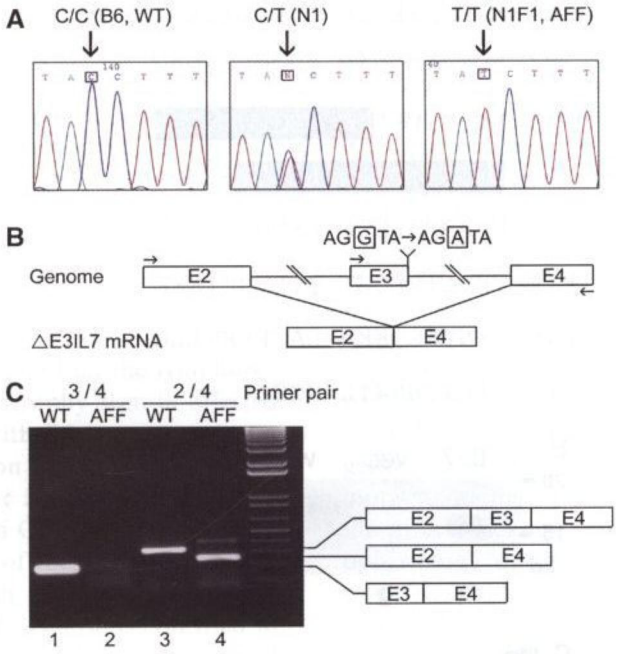

Figure 5. A point mutation at the splicing donor site of the IL-7 gene causes exon 3 skipping.(**A**) Direct sequencing of the exon/intron junction of the exon 3 with a reverse primer. The nucleotide mutated by ENU is shown in a box. (**B**) Schematic representation of the exon 3 skipping in mRNA caused by genomic mutation at the splicing donor site. The boxed nucleotide is the site of mutation wherein the GT consensus dinucleotide was changed to AT. (**C**) The exon 3 skipping phenomenon was revealed by RT-PCR. The positions of the primer pairs used are depicted as arrows in panel B. The structures of these PCR products are schematically represented.

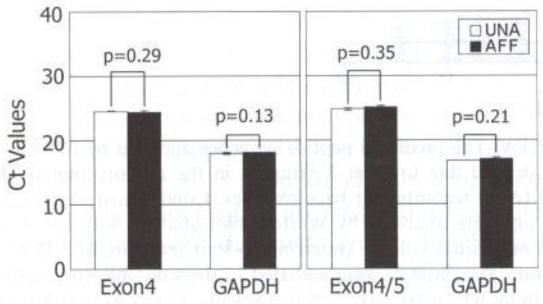

Figure 6. Quantification of ΔE3-IL-7 mRNA by real-time RT-PCR. The total RNA was isolated from unaffected and affected mouse thymus and equal amount of mRNA was subjected to real-time RT-PCR analysis. The *Ct* values were determined according to the instruction of ABI com. Values were average ± SD of three independent RNA preparations. The exon 4 primer set is to determine the level of total RNA, whereas the exon 4/5 primer set is to determine the level of spliced mature RNA. None of these *p* values show a significant difference between the levels of IL-7 mRNA in unaffected and affected animals.

It is worth noting that skipping of exon 3 does not interrupt the IL-7 mRNA reading frame. The ΔE3-IL-7 cDNA thus can potentially encode a 127-aa polypeptide that lacks a sequence from aspartic acid-49 to lysine-75, according to sequence annotation (highlighted region, Figure 7A). To demonstrate the ability of this mutant cDNA to encode a polypeptide, we subcloned wt- or ΔE3-IL-7 cDNA into a baculoviral transfer vector pVL1393 and recombined it with the BaculoGold viral DNA to produce the recombinant virus (see "Materials and Methods"). As shown in Figure 7B, Western blot analysis using IL-7 specific antibody revealed that conditioned media from SF21AE cells infected with the wt-IL-7 recombinant virus gave a specific signal of 17-kDa (Figure 7B, lane 3), which was quite similar to the 16-kDa signal appeared in a lane loaded with a positive control, i.e. bacterially produced recombinant IL-7 purchased from a commercial source (R&D) (Figure 7B, lane 1). Under the same conditions, the ΔE3-IL-7 virus produced a protein of 14-kDa that could be specifically recognized by the IL-7 antibody (Figure 7B, lane 4), suggesting that the ΔE3-IL-7 cDNA can indeed encode a polypeptide. Next, we examined whether the truncated ΔE3-IL-7 protein would retain any known activity of the

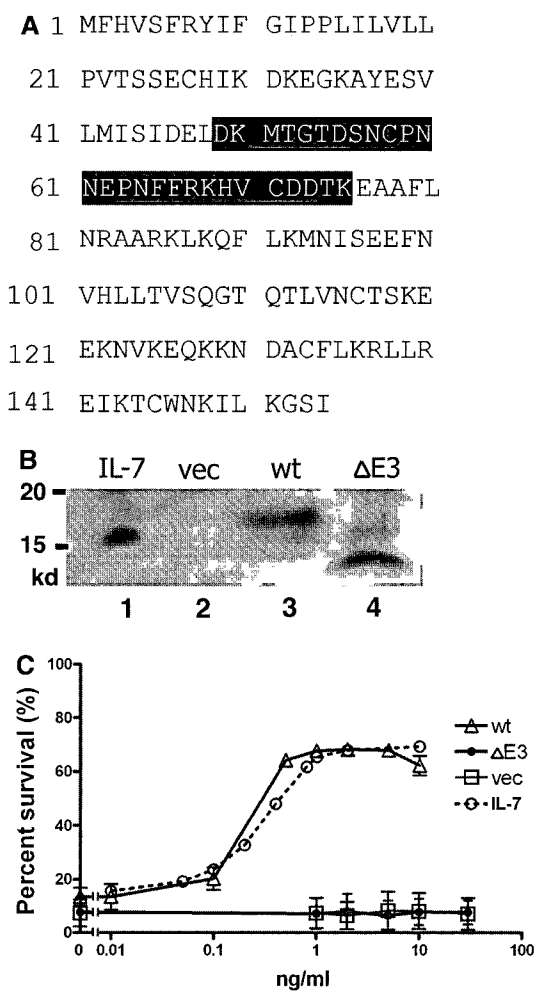

Figure 7. Production and characterization of an internal truncated IL-7. (**A**) The predicted peptide sequence encoded by full-length wild-type IL-7 mRNA. The highlighted region indicates the sequence deleted due to exon 3 skipping in the mutant animal. (**B**) Western blot analysis of IL-7 produced by wild-type- (wt) or ΔE3-IL-7 (ΔE3) recombinant baculoviruses. Conditioned media containing equal amounts of baculovirus-produced wt- or ΔE3-IL-7 (~0.8 μg) were analyzed by Western blot analysis with anti-murine IL-7 antibody. Half μg of bacterially produced IL-7 (IL-7, lane 1) and equal volume (referring to that used for ΔE3-IL7) of conditioned medium from a control virus expressing an irrelevant protein (Vec, lane 2) were included in the same blot as positive and negative controls, respectively. (**C**) T cell survival in medium containing wt- or ΔE3-IL-7. Naïve splenic T cells were cultivated in medium supplemented with various amounts of those four proteins as described in panel B. Ninety-six hours later, cells that had undergone apoptosis were analyzed by the annexin V staining assay, and the percentage of cells that had survived after each treatment (annexin V-negative) was plotted against the amounts of proteins used in the assay. As a negative control, for each dose tested for ΔE3-IL-7, an equal volume of control conditioned medium (Vec, see panel B) was used in this assay. The plotted values shown in the figure were mean ± SD (n = 3).

wild-type protein. To address this issue, we employed the naïve splenic T cell survival assay [28] and baculovirus-produced proteins to compare the anti-apoptotic activity of both wt and mutant IL-7. For this assay, conditioned medium from recombinant virus-infected insect cells were first quantified by ELISA and equal amounts of wt or mutant IL-7 were then added to freshly isolated naïve splenic T cells. Four days later, survival of these T cells were quantified by subtracting those that had undergone apoptosis, which was analyzed by the annexin V binding assay. As shown in Figure 7C, with a dose ranging from 0.01 to 10 ng/ml, the apoptosis suppressing activity of wt-IL-7 produced by the recombinant baculovirus (wt) was comparable to that produced by a bacterial system (IL-7), both with an ED50 of approximately 0.3–0.4 ng/ml. In contrast, with all

doses tested (0–30 ng/ml), the ΔE3-IL-7 protein (ΔE3) failed to manifest any apoptosis suppressing activity that was significantly higher than the background activity observed with an equal volume of conditioned medium from insect cells infected with a control virus producing an irrelevant protein XylE (vec).

Discussion

In this study, we demonstrate that the lymphopenia and lymphoid organ atrophy seen in affected G3 mice only correlate with B6 homozygosity at the chromosome 3A region of the genome in the N1F1 generation. Further analysis of this chromosomal region revealed a G to A point mutation in the splicing donor site of the third exon of the IL-7 genomic locus. In fact, we have continued to outcross affected mice to C3H strains and tried to genotype affected animals based on detection of such a point mutation. Up to the N3F1 generation with 10 1 of mice analyzed, we have not encountered any exception to the rule that the lymphopenia phenotypes always match the point mutation genotype at the IL-7 genomic locus. This result suggests that there are no contributions from other genes to the affected phenotype, as most other ENU mutations in G3 mice should have been diluted out during multiple outcrosses.

The lymphopenia phenotype of our ENU mutant mice is apparently less severe than that reported for the IL-7-gene knockouts. For examples, in the knockouts, no, instead of smaller, lymph nodes were detected, and a much more reduction of thymus and spleen cellularity was observed (<5 and 15% of that of controls, respectively) [12]. This suggests that the G to A point mutation detected in this study has rendered the IL-7 gene to be a hypomorphic allele, a conclusion seemingly contradicts with that reached from the experiment showing that the ΔE3-IL-7 protein failed to manifest any significant anti-apoptotic activity. Our best interpretation for these results is as follows. First, although under our experimental conditions we cannot detect any T cell survival activity of the ΔE3-IL-7 protein, we cannot rule out the possibility that this mutant protein still has a residual activity *in vivo*, which can support the survival of a low percentage of lymphocytes. On the other hand, the mutation in the splicing donor site may not completely abolish the normal splicing event and trace amounts of wild-type IL-7 mRNA and proteins are still made in some tissues whose levels are too low to be detected by our assay methods. Either or both of these two scenarios will result in a mutant mouse with an IL-7-hypomorphic phenotype. Alternatively, what we have observed in this study could be indeed an IL-7-null phenotype. However, it is less severe in our mutant mice with a C56BL/6-C3H mixed genetic background than in the reported IL-7 knockouts that were apparently with a 129/sv-B6 mixed background [12].

Although the IL-7 gene-targeting mouse was generated many years ago [12], our IL-7 point mutation animals provide several advantages over the gene knockout mouse model. First, the pathophysiology of these mutant mice more closely resembles the human disease, as the human disease is most frequently caused by point mutations. In addition, the mutant mouse will least likely mount an immune reaction against the recombinant murine IL-7, since affected mice still produce IL-7 protein, albeit being a non-functional variant. Furthermore, this mutant phenotype has been maintained in the inbred B6 background (G5 and G7 mice, data not shown). This feature may facilitate immunological studies where an inbred mouse genetic background is required. The present study successfully demonstrates how a traditional genetic study can be performed, utilizing advances in genome knowledge and technology as a platform, to improve the speed, convenience and production of a novel research model.

Our SNP genotyping revealed that of the nearly 200 mice that were analyzed, only two had genetic crossover between marker #42 and the affected allele (i.e. the mutated gene). One of the mice exhibiting genetic crossover in this region was an affected mouse that was heterozygous and the other was an unaffected mouse that was homozygous at marker #42 (data not shown). These observations suggest that the mutation site is about 1 cM (equivalent to 2 Mb) away from marker #42 and is estimated to be located at 7.6 Mb in chromosome 3. Note that this number is very close to the physical position of the IL-7 gene, which is located at 7.5 Mb of chromosome 3, according to the NIH mouse genome program (http://www.ncbi.nlm.nih.gov/genome/guide/mouse/).

A G-to-A point mutation was identified at the exon 3 splicing donor site of the IL-7 gene, abolishing the GT dinucleotide consensus sequence motif and causing exon 3 skipping in mRNA maturation. Interestingly, this aberrant ΔE3-IL-7 mRNA does not alter mRNA stability, but can still encode an internally truncated IL-7 protein. We could not compare the endogenous protein level of truncated IL-7 to that of wild-type protein by either Western blot or ELISA due to the extremely low abundance of IL-7. This paucity of IL-7 is consistent with our and others previous observations that the heterozygous animals show a significant reduction in the number of B lymphocytes [29] and T lymphocytes (data not shown).

Acknowledgements

We are grateful to Jia-Zu Chen, Wan-Chen Hsieh, Chien-Tsang Sun and Yoo-Hsan Lin for their technical assistance, and to Drs. Yuan-Tsong Chen, Chien-Kuo Lee, and Hsin-Fang Yang-Yen for their critical reading of this manuscript. We thank the ENU mutagenesis core for providing G3 mice and the National Genotyping center for technical support. This work was supported by the Genomics and Proteomics Program from Academia Sinica, Taiwan to JJY.

References

1. Waterston R.H., Lindblad-Toh K., Birney E., Rogers J., Abril J.F., Agarwal P., Agarwala R., Ainscough R., Alexandersson M., An P., Antonarakis S.E., Attwood J., Baertsch R., Bailey J., Barlow K., Beck S., Berry E., Birren B., Bloom T., Bork P., Botcherby M., Bray N., Brent M.R., Brown D.G., Brown S.D., Bult C., Burton J., Butler J., Campbell R.D., Carninci P., Cawley S., Chiaromonte F., Chinwalla A.T., Church D.M., Clamp M., Clee C., Collins F.S., Cook L.L., Copley R.R., Coulson A., Couronne O., Cuff J., Curwen V., Cutts T., Daly M., David R., Davies J., Delehaunty K.D., Deri J., Dermitzakis E.T., Dewey C., Dickens N.J., Diekhans M., Dodge S., Dubchak I., Dunn D.M., Eddy S.R., Elnitski L., Emes R.D., Eswara P., Eyras E., Felsenfeld A., Fewell G.A., Flicek P., Foley K., Frankel W.N., Fulton L.A., Fulton R.S., Furey T.S., Gage D., Gibbs R.A., Glusman G., Gnerre S., Goldman N., Goodstadt L., Grafham D., Graves T.A., Green E.D., Gregory S., Guigo R., Guyer M., Hardison R.C., Haussler D., Hayashizaki Y., Hillier L.W., Hinrichs A., Hlavina W., Holzer T., Hsu F., Hua A., Hubbard T., Hunt A., Jackson I., Jaffe D.B., Johnson L.S., Jones M., Jones T.A., Joy A., Kamal M., Karlsson E.K., Karolchik D., Kasprzyk A., Kawai J., Keibler E., Kells C., Kent W.J., Kirby A., Kolbe D.L., Korf I., Kucherlapati R.S., Kulbokas E.J., Kulp D., Landers T., Leger J.P., Leonard S., Letunic I., Levine R., Li J., Li M., Lloyd C., Lucas S., Ma B., Maglott D.R., Mardis E.R., Matthews L., Mauceli E., Mayer J.H., McCarthy M., McCombie W.R., McLaren S., McLay K., McPherson J.D., Meldrim J., Meredith B., Mesirov J.P., Miller W., Miner T.L., Mongin E., Montgomery K.T., Morgan M., Mott R., Mullikin J.C., Muzny D.M., Nash W.E., Nelson J.O., Nhan M.N., Nicol R., Ning Z., Nusbaum C., O'Connor M.J., Okazaki Y., Oliver K., Overton-Larty E., Pachter L., Parra G., Pepin K.H., Peterson J., Pevzner P., Plumb R., Pohl C.S., Poliakov A., Ponce T.C., Ponting C.P., Potter S., Quail M., Reymond A., Roe B.A., Roskin K.M., Rubin E.M., Rust A.G., Santos R., Sapojnikov V., Schultz B., Schultz J., Schwartz M.S., Schwartz S., Scott C., Seaman S., Searle S., Sharpe T., Sheridan A., Shownkeen R., Sims S., Singer J.B., Slater G., Smit A., Smith D.R., Spencer B., Stabenau A., Stange-Thomann N., Sugnet C., Suyama M., Tesler G., Thompson J., Torrents D., Trevaskis E., Tromp J., Ucla C., Ureta-Vidal A., Vinson J.P., Von Niederhausern A.C., Wade C.M., Wall M., Weber R.J., Weiss R.B., Wendl M.C., West A.P., Wetterstrand K., Wheeler R., Whelan S., Wierzbowski J., Willey D., Williams S., Wilson R.K., Winter E., Worley K.C., Wyman D., Yang S., Yang S.P., Zdobnov E.M., Zody M.C. and Lander E.S., Initial sequencing and comparative analysis of the mouse genome. Nature 420: 520–562, 2002.
2. Herron B.J., Lu W., Rao C., Liu S., Peters H., Bronson R.T., Justice M.J., McDonald J.D. and Beier D.R., Efficient generation and mapping of recessive developmental mutations using ENU mutagenesis. Nat. Genet 30: 185–189, 2002.
3. Hrabe de Angelis M.H., Flaswinkel H., Fuchs H., Rathkolb B., Soewarto D., Marschall S., Heffner S., Pargent W., Wuensch K., Jung M., Reis A., Richter T., Alessandrini F., Jakob T., Fuchs E., Kolb H., Kremmer E., Schaeble K., Rollinski B., Roscher A., Peters C., Meitinger T., Strom T., Steckler T., Holsboer F., Klopstock T., Gekeler F., Schindewolf C., Jung T., Avraham K., Behrendt H., Ring J., Zimmer A., Schughart K., Pfeffer K., Wolf E. and Balling R., Genome-wide, large-scale production of mutant mice by ENU mutagenesis. Nat. Genet 25: 444–447, 2000.
4. Kile B.T., Hentges K.E., Clark A.T., Nakamura H., Salinger A.P., Liu B., Box N., Stockton D.W., Johnson R.L., Behringer R.R., Bradley A. and Justice M.J., Functional genetic analysis of mouse chromosome 11. Nature 425: 81–86, 2003.
5. Nolan P.M., Peters J., Strivens M., Rogers D., Hagan J., Spurr N., Gray I.C., Vizor L., Brooker D., Whitehill E., Washbourne R., Hough T., Greenaway S., Hewitt M., Liu X., McCormack S., Pickford K., Selley R., Wells C., Tymowska-Lalanne Z., Roby P., Glenister P., Thornton C., Thaung C., Stevenson J.A., Arkell R., Mburu P., Hardisty R., Kiernan A., Erven A., Steel K.P., Voegeling S., Guenet J.L., Nickols C., Sadri R., Nasse M., Isaacs A., Davies K., Browne M., Fisher E.M., Martin J., Rastan S., Brown S.D. and Hunter J., A systematic, genome-wide, phenotype-driven mutagenesis programme for gene function studies in the mouse. Nat. Genet. 25: 440–443, 2000.
6. Hoebe K., Du X., Georgel P., Janssen E., Tabeta K., Kim S.O., Goode J., Lin P., Mann N., Mudd S., Crozat K., Sovath S., Han J. and Beutler B., Identification of Lps2 as a

key transducer of MyD88-independent TIR signalling. Nature 424: 743–748, 2003.
7. Jun J.E., Wilson L.E., Vinuesa C.G., Lesage S., Blery M., Miosge L.A., Cook M.C., Kucharska E.M., Hara H., Penninger J.M., Domashenz H., Hong N.A., Glynne R.J., Nelms K.A. and Goodnow C.C., Identifying the MAGUK protein Carma-1 as a central regulator of humoral immune responses and atopy by genome-wide mouse mutagenesis. Immunity 18: 751–762, 2003.
8. Vitaterna M.H., King D.P., Chang A.M., Kornhauser J.M., Lowrey P.L., McDonald J.D., Dove W.F., Pinto L.H., Turek F.W. and Takahashi J.S., Mutagenesis and mapping of a mouse gene, Clock, essential for circadian behavior. Science 264: 719–725, 1994.
9. Namen A.E., Lupton S., Hjerrild K., Wignall J., Mochizuki D.Y., Schmierer A., Mosley B., March C.J., Urdal D. and Gillis S., Stimulation of B-cell progenitors by cloned murine interleukin-7. Nature 333: 571–573, 1988.
10. Murray R., Suda T., Wrighton N., Lee F. and Zlotnik A., IL-7 is a growth and maintenance factor for mature and immature thymocyte subsets. Int. Immunol. 1: 526–531, 1989.
11. Maeurer M.J. and Lotze M.T., Interleukin-7 (IL-7) knockout mice. Implications for lymphopoiesis and organ-specific immunity. Int. Rev. Immunol. 16: 309–322, 1998.
12. von Freeden-Jeffry U., Vieira P., Lucian L.A., McNeil T., Burdach S.E. and Murray R., Lymphopenia in interleukin (IL)-7 gene-deleted mice identifies IL-7 as a nonredundant cytokine. J. Exp. Med. 181: 1519–1526, 1995.
13. Peschon J.J., Morrissey P.J., Grabstein K.H., Ramsdell F.J., Maraskovsky E., Gliniak B.C., Park L.S., Ziegler S.F., Williams D.E., Ware C.B., Meyer J.D. and Davison B.L., Early lymphocyte expansion is severely impaired in interleukin 7 receptor-deficient mice. J. Exp. Med. 180: 1955–1960, 1994.
14. Macchi P., Villa A., Giliani S., Sacco M.G., Frattini A., Porta F., Ugazio A.G., Johnston J.A., Candotti F., O'Shea J.J. *et al, Mutations of Jak-3 gene in patients with autosomal severe combined immune deficiency (SCID). Nature 377*: 65–68, 1995.
15. Noguchi M., Yi H., Rosenblatt H.M., Filipovich A.H., Adelstein S., Modi W.S., McBride O.W. and Leonard W.J., Interleukin-2 receptor gamma chain mutation results in X-linked severe combined immunodeficiency in humans. Cell 73: 147–157, 1993.
16. Puck J.M., Deschenes S.M., Porter J.C., Dutra A.S., Brown C.J., Willard H.F. and Henthorn P.S., The interleukin-2 receptor gamma chain maps to Xq13.1 and is mutated in X-linked severe combined immunodeficiency, SCIDX1. Hum. Mol. Genet. 2: 1099–1104, 1993.
17. Puel A., Ziegler S.F., Buckley R.H. and Leonard W.J., Defective IL7R expression in T(−)B(+)NK(+) severe combined immunodeficiency. Nat. Genet. 20: 394–397, 1998.
18. Russell S.M., Tayebi N., Nakajima H., Riedy M.C., Roberts J.L., Aman M.J., Migone T.S., Noguchi M., Markert M.L., Buckley R.H., O'Shea J.J. and Leonard W.J., Mutation of Jak3 in a patient with SCID: essential role of Jak3 in lymphoid development. Science 270: 797–800, 1995.
19. Weber J.S., Salinger A. and Justice M.J., Optimal N-ethyl-N-nitrosourea (ENU) doses for inbred mouse strains. Genesis 26: 230–233, 2000.
20. Huang H.M., Li J.C., Hsieh Y.C., Yang-Yen H.F. and Yen J.J., Optimal proliferation of a hematopoietic progenitor cell line requires either costimulation with stem cell factor or increase of receptor expression that can be replaced by overexpression of Bcl-2. Blood 93: 2569–2577, 1999.
21. Yu Y.L., Chiang Y.J. and Yen J.J., GATA factors are essential for transcription of the survival gene E4bp4 and the viability response of interleukin-3 in Ba/F3 hematopoietic cells. J. Biol. Chem. 277: 27144–27153, 2002.
22. Pletcher M.T., McClurg P., Batalov S., Su A.I., Barnes S.W., Lagler E., Korstanje R., Wang X., Nusskern D., Bogue M.A., Mural R.J., Paigen B. and Wiltshire T., Use of a dense single nucleotide polymorphism map for in silico mapping in the mouse. PLoS Biol. 2: e393, 2002.
23. Jurinke C., van den Boom D., Cantor C.R. and Koster H., The use of MassARRAY technology for high throughput genotyping. Adv. Biochem. Eng. Biotechnol. 77: 57–74, 2002a.
24. Jurinke C., van den Boom D., Cantor C.R. and Koster H., Automated genotyping using the DNA MassArray technology. Methods Mol. Biol. 187: 179–192, 2002b.
25. Yuan H.Y., Chen J.J., Lee M.T., Wung J.C., Chen Y.F., Charng M.J., Lu M.J., Hung C.R., Wei C.Y., Chen C.H., Wu J.Y. and Chen Y.T., A novel functional VKORC1 promoter polymorphism is associated with inter-individual and inter-ethnic differences in warfarin sensitivity. Hum. Mol. Genet. 14: 1745–1751, 2005.
26. Schmittgen T.D. and Zakrajsek B.A., Effect of experimental treatment on housekeeping gene expression: validation by real-time, quantitative RT-PCR. J. Biochem. Biophys. Methods 46: 69–81, 2000.
27. Wu J.Y., Kao H.J., Li S.C., Stevens R., Hillman S., Millington D. and Chen Y.T., ENU mutagenesis identifies mice with mitochondrial branched-chain aminotransferase deficiency resembling human maple syrup urine disease. J. Clin. Invest. 113: 434–440, 2004.
28. Rathmell J.C., Farkash E.A., Gao W. and Thompson C.B., IL-7 enhances the survival and maintains the size of naive T cells. J. Immunol. 167: 6869–6876, 2001.
29. Oliver P.M., Wang M., Zhu Y., White J., Kappler J. and Marrack P., Loss of Bim allows precursor B cell survival but not precursor B cell differentiation in the absence of interleukin 7. J. Exp. Med. 200: 1179–1187, 2004.